AAC Accepted Manuscript Posted Online 17 August 2020 Antimicrob. Agents Chemother. doi:10.1128/AAC.00363-20 Copyright © 2020 American Society for Microbiology. All Rights Reserved.

1	Rifabutin is bactericidal against intracellular and extracellular forms
2	of Mycobacterium abscessus
3	
4	
5	Matt D. Johansen ¹ , Wassim Daher ^{1,2} , Françoise Roquet-Banères ¹ , Clément Raynaud ¹ ,
6	Matthéo Alcaraz ¹ , Florian P. Maurer ^{3,4} , and Laurent Kremer ^{1,2,#}
7	
8	
9	¹ Centre National de la Recherche Scientifique UMR 9004, Institut de Recherche en Infectiologie de
10	Montpellier (IRIM), Université de Montpellier, 1919 route de Mende, 34293, Montpellier, France.
11	² INSERM, IRIM, 34293 Montpellier, France.
12	³ National and WHO Supranational Reference Center for Mycobacteria, Research Center Borstel-
13	Leibniz Lung Center, 23845 Borstel, Germany.
14	⁴ Institute of Medical Microbiology, Virology and Hygiene, University Medical Center Hamburg
15	Eppendorf, Hamburg, Germany
16	
17	
18	
19	*To whom correspondence should be addressed:
20	Tel: (+33) 4 34 35 94 47; E-mail: laurent.kremer@irim.cnrs.fr
21	
22	
23	
24	Running title: In vivo efficacy of rifabutin against M. abscessus
25	
26	
27	Keywords: Mycobacterium abscessus, rifabutin, macrophage, zebrafish, therapeutic activity.
28	

Downloaded from http://aac.asm.org/ on August 22, 2020 at Dana Medical Library, University of Vermont

ABSTRACT

30

29

31

32

33

34

35

36

37

38

39

40

41

42

43 44

45

46 47

48

Mycobacterium abscessus is increasingly recognized as an emerging opportunistic pathogen causing severe lung diseases. As it is intrinsically resistant to most conventional antibiotics, there is an unmet medical need for effective treatments. Repurposing of clinically validated pharmaceuticals represents an attractive option for the development of chemotherapeutic alternatives against M. abscessus infections. In this context, rifabutin (RFB) has been shown to be active against M. abscessus and has raised renewed interest in using rifamycins for the treatment of M. abscessus pulmonary diseases. Herein, we compared the in vitro and in vivo activity of RFB against the smooth and rough variants of M. abscessus, differing in their susceptibility profile to several drugs and physiopathologial characteristics. While the activity of RFB is greater against rough strains than in smooth strains in vitro, suggesting a role of the glycopeptidolipid layer in susceptibility to RFB, both variants were equally susceptible to RFB inside human macrophages. RFB treatment also led to a reduction in the number and size of intracellular and extracelluar mycobacterial cords. Furthermore, RFB was highly effective in a zebrafish model of infection and protected the infected larvae from M. abscessusinduced killing. This was corroborated with a significant reduction in the overall bacterial burden, as well as decreased numbers of abscesses and cords, two major pathophysiological traits in infected zebrafish. This study indicates that RFB is active against M. abscessus both in vitro and in vivo, further supporting its potential usefulness as part of combination regimens targeting this difficult-to-treat mycobacterium.

INTRODUCTION

50 51

49

52

53

54

55

56

57

58

59

60

61

62

63 64

65

66

67

68 69

70

71

72 73

74

75

76

77

78

Nontuberculous mycobacteria (NTM) are environmental mycobacteria. Among all NTM, Mycobacterium avium and Mycobacterium abscessus represent the most frequent pathogens associated with pulmonary disease (1). M. abscessus is a rapidly growing NTM of increasing clinical significance, particularly in cystic fibrosis (CF) patients (2). In CF patients, infection with M. abscessus correlates with a more rapid decline in lung function and can represent an obstacle to subsequent lung transplantation (3-5). From a taxonomical view, the species currently comprises three subspecies: M. abscessus subsp. abscessus (designated hereafter M. abscessus), M. abscessus subsp. bolletii (designated hereafter M. bolletii) and M. abscessus subsp. massiliense (designated hereafter M. massiliense) (6). These subspecies exhibit different clinical outcomes and drug susceptible profiles to antibiotic treatments (7).

M. abscessus strains can exhibit either a smooth (S) or rough (R) morphotype as a consequence of the presence or absence, respectively, of bacterial surface glycopeptidolipids (GPL) (1, 8-10). These morphological distinctions are associated with important physiological differences. S variants are more hydrophilic than R variants, enabling increased sliding motility and the capacity to form biofilms (8, 9, 11), while the aggregative R variants possess a high propensity to produce large bacterial cords (11, 12). While S and R variants can be viewed as two representatives of the same isolate, which can co-exist and evolve differently in response to host immunity, they express different pathophysiological traits (10). S variants are typically less virulent than the R variants (11, 13, 14), the latter being more frequently associated with severe lung diseases and persisting for years in CF patients (3, 5). Importantly, an S-to-R transition within the colonized host (5, 15) is linked to genetic polymorphisms within the GPL biosynthetic/transport locus (15, 16). Moreover, differences in the susceptibility to drug candidates have been identified between S and R variants (17, 18), highlighting the need for the improved evaluation of new compounds/drug regimens against both morphotypes.

Treatment of M. abscessus lung disease remains particularly challenging, largely due to intrinsic resistance to wide panel of antimicrobial agents, including most antitubercular drugs such as rifampicin (RIF) (19-22). The extensive resistome of M. abscessus results from a low permeability of the cell wall, absence of drug-activating systems, induction of efflux pumps and production of a wide panel of drug-modifying enzymes (19, 22, 23). In addition, mutations in genes encoding drug targets

81 82

83

84 85

86

87 88

89

90

91

92

93

94

95

96 97

98

99

100

101

102

can result in acquired drug resistance further complicating therapy (1, 24). Treatment of infections caused by M. abscessus require prolonged courses of multiple antibiotics, usually combining a macrolide (azithromycin or clarithomycin), a β-lactam (imipenem or cefoxitin) and an aminoglycoside (amikacin) (25, 26, 27). Additional drugs, such as tigecycline or clofazimine, are often added to strengthen the regimen, particularly in response to toxic side effects or unsatisfactory clinical response (28). Despite intensive chemotherapy, treatment success rates typically remain around 25-40% in the case of macrolide resistance, which occurs in at least 40-60% of clinical isolates (29). Therefore, there is an urgent clinical need for new drug regimens with improved efficacy (30). While the current drug pipeline against M. abscessus remains poor, it has recently been fueled with the discovery of several active hits and the development of repurposed drugs (24). Among the latter, screening of libraries of approved pharmaceuticals revealed that rifabutin (RFB), a rifamycin related to the poorly active rifampicin (RIF), shows activity against M. abscessus (31, 32). RIF, along with many other rifamycins, is inactivated by the ADP-ribosyltransferase (Arr_{Mab}) encoded by MAB 0591, which ribosylates the drug at the C23 hydroxyl position (33). RFB has also been reported to be as active as clarithromycin in immune-compromized NOD/SCID mice infected with M. abscessus (34). However, most studies on RFB have been carried out on either S or R variants (when reported), rendering results sometimes difficult to interpret and/or to compare. Due to the co-existence of S and R variants in patients (15) and the presence of each variant in different compartments (S residing mostly in macrophages and R growing also in the form of intra- or extracellular cords), it is essential to address the activity of RFB on isogenic S/R pairs in both in vitro and in vivo studies.

The present study aimed to describe and compare the activity of RFB against S and R M. abscessus complex strains in vitro and ex vivo in a macrophage infection model. Due to the importance of cording, considered as a marker of severity of the infection with the R variant, we also investigated the efficacy of RFB in a zebrafish model of infection.

MATERIALS AND METHODS

104 105

106

107

108

109

110 111

112

113

103

Mycobacterial strains and growth conditions. M. abscessus CIP104536^T, M. bolletii CIP108541^T and M. massiliense CIP108297^T reference strains and clinical isolates from CF and non-CF patients were reported previously (35, 36). Strains were routinely grown and maintained at 30°C in Middlebrook 7H9 broth (BD Difco) supplemented with 0.05% Tween 80 (Sigma-Aldrich) and 10% oleic acid, albumin, dextrose, catalase (OADC enrichment; BD Difco) (7H9^{T/OADC}) or on Middlebrook 7H10 agar (BD Difco) containing 10% OADC enrichment (7H10^{OADC}) and in the presence of antibiotics, when required. For drug susceptibility testing, bacteria were grown in Cation-Adjusted Mueller-Hinton Broth (CaMHB; Sigma-Aldrich). RFB was purchased from two independent commercial sources (Adooq Bioscience and Selleckchem) and dissolved in DMSO.

114 115

116

117

118 119

120

121

122

Drug susceptibility testing. The minimal inhibitory concentrations (MIC) were determined according to the CLSI guidelines (37). The broth micro-dilution method was used in CaMHB with an inoculum of 5x10⁶ CFU/mL in exponential growth phase. The bacterial suspension was seeded in 100 μL volumes in all of the wells of a 96-well plate, except for the first column, to which 198 μL of the bacterial suspension was added. In the first column, 2 µL of drug at its highest concentration was added to the first well containing 198 µL of bacterial suspension. Two-fold serial dilutions were then carried out and the plates were incubated for 3-5 days at 30°C. MICs were recorded by visual inspection. Assays were completed in triplicate in three independent experiments.

123 124

125

126 127

Growth inhibition kinetics. To monitor growth inhibition of *M. abscessus* CIP104536^T S and R, 96-well plates were set-up as for MIC determination and serial dilutions of the bacterial suspensions exposed to increasing concentrations of RFB were plated on LB agar plates after 0, 24, 48 and 72 hrs. Colonyforming units (CFUs) were counted after 4 days of incubation at 30°C. Results from each drug concentration are representative of at least 2 independent experiments.

128 129 130

131

132

Cytotoxicity assay. THP-1 cells were differentiated with PMA for 48 hrs and exposed to decreasing concentrations of either RFB or RIF (starting at 200 µg/mL) for an additional 72 hrs at 37°C with 5% CO₂. Following incubation, 10% (vol/vol) resazurin dye was added to each well and left to incubate for 4 hrs at 37°C and 5% CO₂. Data was acquired using a fluorescent plate reader (excitation 540 nm, emission 590 nm). DMSO was included as a negative control, while SDS was included as a positive control.

135 136 137

138

139

140

141

142

143

144

145

146

147

133 134

> Intracellular killing assay. Human THP-1 monocytes were grown in RPMI medium supplemented with 10% Fetal bovine serum (Sigma Aldrich) (RPMI^{FBS}) and incubated at 37°C in the presence of 5% CO₂. Cells were differentiated into macrophages in the presence of 20 ng/mL Phorbol Myristate Acetate (PMA) in 24-well flat-bottom tissue culture microplates (10⁵ cells/mL) and incubated for 48 hrs at 37°C with 5% CO₂. Infection with clinical isolates or M. abscessus harbouring pTEC27 fluorescent tdTomato was carried out at 37°C in the presence of 5% CO₂ for 3 hrs at a MOI 2:1. After extensive washing with 1X phosphate buffered saline (PBS), cells were incubated with RPMIFBS containing 250 μg/mL amikacin for 2 hrs and washed again with PBS prior to the addition of 500 μL RPMI^{FBS} containing DMSO (negative control) or 500 µL RPMI^{FBS} containing 50 µg/mL of RIF or AMK, or 12.5 μg/mL of RFB. Macrophages were washed with PBS and lysed with 100 μL of 1% Triton X-100 at required time points. Serial dilutions of macrophage lysates were plated onto LB agar plates and colonies were counted to determine intracellular CFUs.

148 149

150

151

152 153

154

155

156 157

158 159

160

161

162

Microscopy-based infectivity assays. Monocytes were differentiated into macrophages (THP-1) in the presence of PMA and were grown on coverslips in 24-well plates at a density of 10⁵ cells/mL for 48 hrs at 37°C with 5% CO₂ prior to infection with Tdtomato expressing M. abscessus for 3 hrs at a MOI of 2:1. After washing and AMK treatment to remove the extracellular bacilli, macrophages were exposed to DMSO (negative control), or 50 μg/mL RIF or AMK, or 12.5 μg/mL RFB, and fixed at 0, 1 and 3 days post-infection with 4% paraformaldehyde in PBS for 20 min. Cells were then permeabilized using 0.2% Triton X-100 for 20 min, blocked with 2% BSA in PBS supplemented with 0.2% Triton X-100 for 20 min, incubated with anti-CD63 antibodies (Becton Dickinson); dilution 1:1000) for 1 hr and with an Alexa Fluor 488-conjugated anti-mouse secondary antibody (Molecular Probes, Invitrogen). After 5 min of incubation with DAPI (dilution 1:1000), cells were mounted onto microscope slides using Immu-mount (Calbiochem) and examined with an epifluorescence microscope using a 63X objective. The average proportion of macrophages containing fewer than <5, 5-10, or >10 bacilli were quantified using Zeiss Axio-vision software. Images were acquired by Downloaded from http://aac.asm.org/ on August 22, 2020 at Dana Medical Library, University of Vermont

focusing on combined signals (CD63 in green and red fluorescent M. abscessus) and captured on a Zeiss Axio-imager confocal microscope equipped with a 63X oil objective and processed using Zeiss Axiovision software. Quantification and scoring of the numbers of bacilli present within macrophages were performed using ImageJ. Equal parameters for the capture and scoring of images were consistently applied to all samples. For each condition, approximately 1000 infected macrophages were analyzed. The presence of the intra- or extracellular cords within or among the macrophages infected with the R morphotype strain were treated in the presence of DMSO, RIF, RFB or AMK at the concentrations previously described, counted and imaged using confocal microscopy.

171 172

173

174

175

176

177

178

179 180

181

182

183

184

185

186 187

188 189

190

191

163 164

165

166

167

168

169

170

Assessment of RFB efficacy in infected zebrafish. Experiments in zebrafish were conducted according to the Comité d'Ethique pour l'Expérimentation Animale de la Région Languedoc Roussillon under the reference CEEALR36-1145. Experiments were performed using the golden mutant (38). Embryos were obtained and maintained as described (14). Embryo age is expressed as hours post fertilisation (hpf). Red fluorescent M. abscessus CIP104536^T (R) expressing tdTomato were prepared and microinjected in the caudal vein (2-3 nL containing ≈100 bacteria/nL) in 30 hpf embryos previously dechorionated and anesthetized with tricaine, as described earlier (39). The bacterial inoculum was checked aposteriori by injection of 2 nL in sterile PBS^T and plating on 7H10^{OADC}. Infected embryos were transferred into 24-well plates (2 embryos/well) and incubated at 28.5°C to monitor kinetics of infection and embryo survival. Survival curves were determined by counting dead larvae daily for up to 12 days, with the experiment concluded when uninfected embryos started to die. RFB treatment of infected embryos and uninfected embryos was commenced at 24 hpi (hours post-infection) for 4 days. The drug-containing solution was renewed daily. Bacterial loads in live embryos were determined by anesthetising embryos in tricaine as previously described (40), mounting on 3% (w/v) methylcellulose solution and taking fluorescent images using a Zeiss Axio Zoom.V16 coupled with an Axiocam 503 mono (Zeiss). Fluorescence Pixel Count (FPC) measurements were determined using the 'Analyse particles' function in ImageJ (39). Bacterial cords were identified based on the size and shape of fluorescent bacteria within the live zebrafish embryo, vastly exceeding the surrounding size and shape of neighbouring cells. All experiments were completed at least three times independently.

192

Downloaded from http://aac.asm.org/ on August 22, 2020 at Dana Medical Library, University of Vermont

219

193 Overexpression of MAB 1409c in M. abscessus. 194 Overexpression was achieved by PCR amplification of MAB 1409c (tap) in fusion with an HA tag using 195 genomic DNA and the forward primer (5'- gagaCAATTGCCATGTCCACTCCGACGGCGGATTC-3'; Mfel) 196 reverse primer gagaGTTAACCTAAGCGTAATCTGGAACATCGTATGGGTACCGAGTTGGTTCCTTGTCGGGCT-3'; Hpal). The 197 amplified product was digested with Mfel/Hpal and ligated into the Mfel/Hpal-restricted pMV306 198 199 integrative vector to generate pMV306-MAB 1409c-HA where MAB 1409c-HA is under the control of 200 the hsp60 promoter. The construct was sequenced and electroporated in M. abscessus S and R. 201 202 Selection of resistant M. abscessus mutants and target identification. Exponentially growing M. abscessus CIP104536^T R cultures were plated on LB agar containing either 25 or 50 μg/mL RFB. After 203 one week of incubation at 37°C, four individual colonies from each RFB concentration were selected, 204 205 grown in CaMHB, individually assessed for MIC determination and scored for resistance to RFB. Identification of SNPs in the resistant strains was completed by PCR amplification using rpoB f 5'-206 207 TCAGTGGGGCTGGTTAG -3' and rpoB r 5'-AAAACATCGCAGATGCGC-3' to produce a 3541 bp amplicon 208 for full coverage sequencing of the rpoB gene. 209 210 Western blotting. Bacteria were harvested, resuspended in PBS, and disrupted by bead-beating with 211 1-mm diameter glass beads. The protein concentration in the lysates was determined and equal 212 amounts of proteins (100 µg) were subjected to SDS/PAGE. Proteins were transferred to a 213 nitrocellulose membrane. For detection of Tap-HA and KasA (loading control), the membranes were 214 incubated for 1 hr with either the rat anti-HA or rat anti-KasA antibodies (dilution 1:2000), washed, and subsequently incubated with goat anti-rat antibodies conjugated to HRP (Abcam, dilution 215 216 1:5000). The signal was revealed using the ChemiDoc MP system (Bio-Rad).

Statistical analyses. Statistical analyses were performed on Prism 5.0 (Graphpad) and detailed for

each figure legend. * $P \le 0.05$, ** $P \le 0.01$, *** $P \le 0.001$, **** $P \le 0.0001$.

RESULTS

221 222

223

224 225

226

227

228

229

230

231

232

233

234

235 236

237

238

239

240

241 242

243

244

245

246 247

248

220

Rough M. abscessus is more susceptible to RFB treatment than smooth M. abscessus in vitro. Exposure of exponentially-growing M. abscessus CIP104536 T S and R isogenic variants to increasing concentrations of RFB, starting at 25 µg/mL for S and 6.25 µg/mL for R, resulted in a noticeable growth inhibition (Fig. 1). At the lowest concentration, the CFUs at 72 hrs post-treatment remained comparable to those of the inoculum, suggestive of a bacteriostatic effect. However, the highest RFB concentrations for both S (200 µg/mL) and R (50 µg/mL) variants were accompanied by 1.81 and 2.47 Log reduction in the CFU counts at 72 hrs post-treatment, respectively (Fig. 1). While similar bactericidal effects of RFB were observed against both variants, this was achieved with lower concentrations of RFB against the R variant relative to the isogenic S variant. Overall, RFB at concentratios of 12.50 µg/mL (For R) resulted in a killing effect comparable to the one of imipenem (IPM) used at the MIC (16 μ g/mL), known as an active β -lactam drug against M. abscessus (41) (Fig. 1).

To confirm the differences in the susceptibility to RFB, we determined the MIC of the CIP104536^T S and R variants in CaMHB. Table 1 clearly shows that the S strain is 4-fold more resistant than its R counterpart. However, both variants were similarly resistant to other rifamycins (RIF, RPT and RFX), in agreement with previous studies (32, 34). Our MIC values, obtained in repetitive experiments with two different commercial sources of RFB, were higher than those reported earlier (32, 34), but comparable to values reported in another study (42). Consistently with other studies (31), we also noticed that the MIC values were dependent on the culture medium (Table S1). Interestingly, MICs of RFB against S and R strains were lower in Middlebrook 7H9 as compared to CaMHB but this effect was lost when supplementing the medium with OADC enrichment. In contrast the S and R strains displayed equal susceptibility levels to RFB in Sauton's medium.

To investigate the relationship between RFB activity and GPL production, drug susceptibility was assessed in CaMHB using the GPL-deficient ΔmmpL4b mutant, generated in the S background of the type strain CIP104536^T, and its complemented counterpart (14, 43, 44). The mmpL4b gene encodes the MmpL4b transporter which participates in the translocation of GPL across the inner membrane (43, 45). Mutations in this gene are associated with loss of GPL and acquisition of a R morphotype (13, 43). The parental S strain and, to a lesser extent the ΔmmpL4b-complemented strain, showed reduced susceptibility to RFB (MIC 32-64 µg/mL) than the M. abscessus R strain and the GPL-deficient ΔmmpL4b mutant (MIC 16 μg/mL) (Table 1). The MIC results are in agreement with the growth inhibition kinetics (Fig. 1) and suggest that the outer GPL layer influences the activity of RFB.

M. abscessus possesses numerous potential drug efflux systems (45), including MAB 1409c, a homolog of Rv1258c, previouly reported to mediate efflux of RIF in M. tuberculosis (46). We thus addressed whether overexpression of MAB 1409c induces resistance to RFB in M. abscessus. MAB 1409c was cloned in frame with a HA-tag in the integrative pMV306. The resulting construct pMV306-MAB 1409c-HA was introduced in both S and R variants and the expression of MAB 1409c was confirmed by Western blot analysis using anti-HA antibodies (Fig. S1). Drug susceptibility assessment indicated a 4-fold upshift in the MIC of RFB against the R strain carrying pMV306-MAB 1409c-HA while no changes in the MIC were observed with the S strain overproducing MAB_1409c (Table 1). This suggests that increasing expression of MAB_1409c in the R variant is likely to mediate efflux of RFB, leading to reduced susceptibility to the drug.

262 263

264

265

266

267

268 269

270

271

272

249

250

251

252

253

254

255

256

257

258

259

260

261

RFB is active against S and R M. abscessus isolates in vitro. The activity of RFB was next tested using a set of clinical strains isolated from CF patients or non-CF patients. In general, the MIC of R strains were 2 to 4 times lower than those of S strains, altough there were variations among the strains (Table 2). Some R strains (10, 112, 179, 210) exhibited higher MIC values (100 µg/mL) than the reference CIP104536^T R strain, while one S strain appeared particularly susceptible to RFB (M. massiliense 120 with a MIC of 6.25 μg/mL). These differences between strains and S/R morphotypes were not observed previously with BDQ and S and R variants were also equally sensitive to BDQ (47). Overall, these results demonstrate that RFB is active against M. abscessus, including isolates from CF patients, while R variants appear in general more susceptible to RFB than S variants, supporting previous findings (48).

273 274 275

276

277

Mutations in rpoB confer resistance to RFB. Although rifamycin resistance mechanisms mediated by mutations in the *rpoB* gene coding for the β-subunit of RNA polymerase have been widely described for M. tuberculosis, this is not the case for M. abscessus. Therefore, to identify the mechanism of

279

280

281

282

283

284 285

286

287

288

289

290

291

292

293

294

295

296

297

298

299

300

301

302

303

304

305

306

resistance of RFB, a genetic approach involving the selection of spontaneous RFB-resistant mutants of M. abscessus followed by rpoB sequencing was applied. Four spontaneous strains were isolated in the presence of 25 or 50 µg/mL RFB, exhibiting 4- to 8-fold increased resistance levels as compared to the parental strain, respectively (Table 3). Sequencing analyses of rpoB identified several single nucleotide polymorphisms (SNPs) across four resistor mutants. In mutants 25.1 and 50.1, a C1339T substitution was identified at position 447 (H447Y). Similarly, in mutant 25.2, a C1339G replacement was found, resulting in an amino acid substitution at position 447 (H447D). Comparatively, in mutant strain 50.2, another SNP (C1355T) occurred, leading to an amino acid change at position 452 (S452L). A comparison of growth of different resistant strains on agar plates containing increasing concentrations of RFB is shown in Fig. S2. Whereas RFB abrogated growth of the wild-type S and R strains, growth of all four resistors harbouring mutations at either positions 447 or 452 sustained bacterial growth at 50 µg/mL, confirming that mutations in rpoB confer resistance to RFB.

M. abscessus S and R strains are equally susceptible to RFB in macrophages. While RFB has been

shown to be active against M. tuberculosis in a macrophage infection model (49), this has not been thoroughly investigated for M. abscessus. We thus compared the intracellular efficacy of RFB in THP-1 macrophages infected with either S or R variants. Firstly, the cytotoxicity of RFB and RIF against THP-1 cells was investigated over a 3-days exposure period to either drug. Fig. S3, clearly shows that RFB exerts significant cytotoxicity at concentration >25 µg/ml and that the kinetic of macrophage killing was more rapid with RFB than with RIF. Based on these results, all subsequent macrophage studies were treated with 50 µg/mL RIF or 12.5 µg/mL RFB. AMK at 50 µg/mL was added as a positive control. DMSO-treated macrophages were included as a negative control for intracellular bacterial replication. At 0, 1 and 3 days post-infection (dpi), macrophages were lysed and plated to determine the intracellular bacterial loads following drug treatment. Whereas the presence of DMSO or RIF failed to inhibit intramacrophage growth of M. abscessus S, exposure to RFB strongly decreased the intracellular bacterial loads at 1 dpi, with this effect further exacerbated at 3 dpi (Fig. 2A). As anticipated, treatment with RIF did not show any effect, in agreement with the poor activity of this compounds in vitro (Table 1). Comparatively, AMK treatment resulted in a significantly reduced intracellular growth rate in both M. abscessus S and R variants between 1 and 3dpi. Interestingly, the

308

309

310

311

312

313

314

315

316

317

318

319

320

321

322

323

324

325

326

327

328

329

331

332 333

334

335

336

RFB susceptibility profile for the S variant at 1 and 3 dpi was comparable to that of the R variant, with a ~3 Log reduction in the CFU counts (Fig. 2A and B, respectively).

Macrophages were next infected with M. abscessus strains expressing Tdtomato and exposed to either DMSO, AMK, RIF or RFB, followed by staining with anti-CD63 and DAPI and observed under a confocal microscope. A quantitative analysis confirmed the marked reduction in the number of M. abscessus S-infected THP-1 cells treated with AMK and RFB at 1 and 3 dpi compared to RIF-treated cells or untreated control cells (Fig. 2C). A similar trend was observed when macrophages were infected with M. abscessus R (Fig. 2D).

Macrophages infected with the S variant were then classified into three categories based on their bacterial burden: poorly infected (<5 bacilli), moderately infected (5-10 bacilli) and heavily infected (>10 bacilli) macrophages. Cells containing bacilli were then individually observed under the microscope and scored to one of the three categories. The quantitative analysis indicates that exposure to RFB significantly reduces the percentage of S variant heavily infected THP-1 cells while increasing the proportion of the poorly infected category, as compared to the untreated cells at 1 dpi (Fig. 2E). At 3 dpi, the effect of RFB was even more pronounced with 10% of the infected bacilli belonging to the heavily infected category and more than 50% associated with the poorly infected category. Analysis performed on cells infected with the R variant generated a similar category profile, although treatment with RFB was associated with a higher proportion of heavily infected macrophages at 3 dpi with the R variant than with the S variant (Fig. 2F). Fig. 2G illustrates the reduced number of M. abscessus S in infected THP-1 cells treated with RFB at 1 dpi, as compared to the untreated control cells (DMSO) or those treated with RIF or AMK. Collectively, these results indicate that RFB enters THP-1 macrophages and similarly impedes bacterial replication of both M. abscessus S and R variants.

330

RFB reduces the intramacrophage growth of clinical isolates. RFB has recently shown vast potential as an effective antibiotic for the treatment of M. abscessus infection in a NOD/SCID murine model (34). However, to date the efficacy of RFB has only been evaluated against a limited panel of M. abscessus clinical isolates within an infection setting. As such, we explored the activity of RFB against S and R clinical isolates of the M. abscessus complex with varying MIC values against RFB within THP-1 macrophages. In support of our previous findings in infected macrophages, RFB treatment (12.5 or

25 μg/mL) was very active against all M. abscessus subspecies within macrophages at 1 and 3 dpi when compared to Day 0 and DMSO treatment (Fig. 3), irrespective of S and R morphotypes and the corresponding MIC values (Table 2). Overall, these findings suggest that RFB is very effective against intracellular clinical isolates and highlights the lack of direct correlation between MICs determined in vitro and the intracellular activity of RFB.

341 342 343

344

345

346

347

348 349

350 351

352

353

337

338 339

340

Reduced intra- and extracellular cording by RFB treatment. An important phenotypic difference between S and R morphotypes is that R morphotypes display increased bacterial aggregation. R bacilli remain attached during replication, forming compact colonies containing structures that resemble cords on agar and in broth medium (8, 12, 14). Fig. 4A clearly shows that, upon infection with M. abscessus R expressing TdTomato, the total number of cords per field was significantly reduced in the presence of 50 µg/mL AMK or 12.5 µg/mL RFB when compared to 50 µg/mL RIF or DMSO alone. Moreover, we observed intracellular cords that are capable of growing inside the macrophage as well as in the extracellular milieu, which were easily observable at 3 dpi (Fig. 4B). As illustrated in Fig. 4C, treatment with AMK or RFB strongly impacted on both intra- and extracellular cords. While AMK treatment severely reduced the number of both intra- and extracellular cords, this effect was almost completely abrogated with RFB at 3 dpi. Together, these results indicate that RFB is highly effective in reducing *M. abscessus* cords, thought to affect the outcome of the infection.

354 355

356

357

358

359

360 361

362

363 364

365

366

RFB treatment enhances protection of zebrafish infected with M. abscessus. In vivo drug efficacy has previously been well described using the zebrafish model of infection (40, 47, 50). Initial experiments indicated that RFB concentrations ≤ 100 µg/mL (final concentration in fish water) did not interfere with larval development and was well tolerated in embryos when treatment was applied for 4 days with daily drug renewal (Fig. 5A). Higher concentrations of RFB, however, were associated with rapid larval death. As such, only lower RFB doses (≤ 100 μg/mL) were used in subsequent studies. Red fluorescent tdTomato-expressing M. abscessus (R variant) was microinjected in the caudal vein of embryos at 30 hrs post-fertilisation (hpf). RFB was directly added at 1 dpi to the water containing the infected embryos, with RFB-supplemented water changed on a daily basis for 4 days. Embryo survival was monitored and recorded daily for 12 days. No decrease in the survival rate was observed in the presence of 5 µg/mL RFB, however, a significant dose-dependent increase in the

survival of embryos exposed to 25 or 50 μg/mL RFB was observed as compared to the untreated group (Fig. 5B). When exposed to 50 µg/mL RFB, the highest dose examined in this setting, nearly 80% of the treated embryos survived at 12 dpi, as compared to 40% of the untreated group. This clearly indicates that RFB protects zebrafish from *M. abscessus* infection.

To test whether RFB exerts an effect on the bacterial burden in zebrafish, we quantified fluorescent pixel counts (FPC) (39). As expected, embryos treated with 50 µg/mL RFB had significantly decreased bacterial burdens at 2, 4 and 6 dpi when compared to the untreated group (Fig. 5C). These results were corroborated by imaging whole embryos, characterised by the presence of large abscesses and cords in the brain when left untreated and which were observed much less frequently in the RFB-treated animals despite the presence of single bacilli or small aggregated bacteria (Fig. 5D).

378 379

380

381

382

383

384

385

386 387

388

389

390 391

367

368

369

370

371

372

373 374

375

376

377

RFB treatment reduces abscess formation by M. abscessus in zebrafish. Virulence of M. abscessus R variants in zebrafish are correlated with the presence of abscesses, particularly in the central nervous system (14, 39). To address whether the enhanced survival of RFB-treated fish is associated with decreased abscess formation, the percentage of abscesses and cords were determined by monitoring abscesses and cords in whole embryos, as reported previously (14, 39). Extracellular cords can be easily distinguished based on their serpentine-like shape and by their size, often greater as compared to the size of the surrounding macrophages and neutrophils. Exposure of infected embryos to 50 µg/mL RFB was accompanied by a significant decrease in the proportion of embryos with cords (Fig. 6A) at 4 dpi, and the number of embryos with abscesses (Fig. 6B) at 4 and 6 dpi. This decrease in the physiopathological signs of RFB-treated larvae correlates also with the FPC analysis and whole embryo imaging (Fig. 6C and 6D). Overall, these results demonstrate that RFB reduces the pathophysiology of M. abscessus infection in zebrafish larvae and protects them from bacterial killing.

DISCUSSION

393

392

394

395

396

397

398

399

400

401

402

403

404

405 406

407

408

409

410

411 412

413

414 415

416

417

418 419

420

421

Treatment success of infections caused by M. abscessus is unacceptably low even upon prolonged, multidrug chemotherapy with a significant risk of severe toxic side effects. Although RIF is used as a first-line drug against M. tuberculosis, it has no activity against M. abscessus. While ADP ribosyltransferases can utilise both RIF and RFB as substrates (51), a lower catalytic efficiency with RFB may explain its greater potency against M. abscessus. Our study supports and extends previous investigations highlighting the potential of RFB against M. abscessus in vitro against a wide panel of M. abscessus complex clinical isolates (31, 32, 52, 53). We found, however, that our MIC values were higher than those observed in previous investigations (31, 32). In our study, following the Clinical and Laboratory Standard Institute (CLSI) guidelines, MIC were determined in CaMHB while Aziz et al. showed that MIC values were 2- to 3-fold higher in CaMHB as compared to Middlebrook 7H9 (31), clearly implicating an effect of medium on RFB susceptibility testing. In line with these results, we noticed important variations in the MIC values depending on the culture medium used for RFB susceptibility assessments. It is also noteworthy that the growth curve of the untreated S strain is different from the one of the R strain, which is very likely linked to the highly aggregative surface properties typifying the R strain which, in contrast to the S strain, produces very clumpy and corded cultures in broth medium (10, 39, 54). As a consequence, colonies on agar plates are very likely emerging from aggregated bacteria rather than individual bacilli, explaining why the CFU counts were significantly lower in both cultures. Thus, the CFU counts of the R strain does not accurately reflect the absolute number of living bacilli in the culture. We also selected RFB-resistant mutants and identified mutations in rpoB, known as the primary target of rifampicin in M. tuberculosis (55). Interestingly, the mutations identified are part of the rifampicin-resistance-determining region (RRDR), a 81-bp central segment corresponding to codons 426 to 452 in M. tuberculsosis that harbours the vast majority of rpoB mutations associated with resistance to RIF (55). Noteworthingly, S452L corresponds to one of the most frequently mutated coding region in the rpoB gene in M. tuberculosis (\$450L replacement) (55). Together, these results suggest RpoB is very likely the target of RFB in M. abscessus.

Among the various studies reporting the activity of RFB against M. abscessus in vitro, very few discriminated the activity of RFB against the S or R morphotypes. Herein, we found that the type

424

425

426

427

428

429

430

431

432

433

434

435 436

437

438

439

440

441 442

443

444

445 446

447

448 449

450

451

strain CIP104536^T S was reproducibly more resistant to RFB than its R counterpart. Supporting these results, deletion of mmpL4b in the S genetic background, resulting into an R morphotype lacking GPL (13, 43), increased susceptibility to RFB. Conversely, functional complementation of the mmpL4b mutant, restoring the S morphotype and GPL production (13, 43), partially rescued the higher MIC. This highlights the influence of the outermost GPL layer on susceptility to RFB. Previously, the activity of other inhibitors have been shown to be dependent on the presence or absence of GPL in M. abscessus (17, 18). A logical explanation is that the GPL layer protects the bacilli from the penetration of drugs. The absence of GPL may enhance the permeability of the cell wall and accumulation of the drug inside the bacteria. However, one cannot exclude the possibility that MmpL4b, like other MmpL transporters, can act as an efflux pump (56–58) and may participate in the extrusion of RFB in M. abscessus S, resulting in higher MIC. The implication of efflux pumps in resistance to RFB has been investigated, whereby the overexpression of MAB 1409c (a homologue of the M. tuberculosis Rv1258c) resulted in increased resistance to RFB in the R variant of M. abscessus. This effect was not observed in the S strain overexpressing MAB_1409c, presumably because of the already elevated MIC of the parental S strain towards RFB. However, while the increased susceptibility of the R strain as compared to the S strain was true with respect to the type strain, this was not observed for all clinical strains tested. The heterogeneity of the clinical strains in response to RFB treatment cannot be simply explained by the presence or absence of GPL, but may also include additional determinants of resistance to RFB (52), such as differences in the expression level of Arr_{Mab} or the expression of Rox monooxygenases, known to inactivate RIF in other bacterial species as proposed earlier (59). This, however, requires further investigation in follow-up studies.

One unanticipated finding from this study relies on the fact that, although S and R variants respond differently to RFB treatment in vitro, this was not the case against the intracellularly-residing M. abscessus. We found that, using a macrophage model of infection, the isogenic S and R type strains responded equally well to treatment with 12.5 µg/mL RFB, largely exceeding the results obtained with AMK, a drug displaying weak intracellular activity (60). These observations are reminiscent of other studies indicating that various naphtalenic ansamycins, including RIF, differ profoundly in their capacity to kill extracellular Staphylococcus aureus, albeit there were few differences observed between them in promoting human macrophages to kill phagocytosed bacteria (61). There is no simple explanation as why M. abscessus S is as efficiently killed as M. abscessus R

453 454

455

456

457

458

459

460

461

462

463

464

465

466 467

468

469

470

471 472

473

474

475 476

477 478

479

480

inside the cells. A plausible explanation may be that the stress response inside macrophages alters the composition/architecture of the cell wall of M. abscessus, thereby affecting the GPL layer and/or permeability of the S variant. It has been shown that the GPL layer significantly influences the hydrophobic surface properties (62), potentially impacting on the adhesion and the uptake of the bacilli. Furthermore, electron microscopy observations revealed that the electron translucent zone (ETZ) that fills the entire space between the phagosome and the bacterial surface relies on GPL production in the S variant (11). Alternatively, RFB may directly induce the antimycobacterial activity of the macrophage, which in turns translates into a rapid killing of the phagocytosed bacteria, regardless of their morphotype. Overall, these results suggest that the MIC values of RFB are not indicative of the intraphagocytic killing of M. abscessus and highlights the importance of testing the efficacy of drugs in a macrophage infection model.

Cords and abscesses are pathophysiological markers of M. abscessus infection, as revealed using the zebrafish model of infection (40). In particular, extracellular cords, due to their size, prevent the bacilli from being phagocytosed by macrophages and neutrophils, representing an important mechanism of immune evasion (14, 39). We demonstrate here that treatment of infected macrophages was associated with reduced intra- and extracellular cording of the R variant. It is very likely that RFB prevents cording, as a consequence of the inhibition of bacterial replication/killing. Cords are a hallmark of virulence of the R variant of M. abscessus, as emphasized by a deletion mutant of MAB_4780, encoding a dehydratase, displaying a pronounced defect in cording and a highly attenuated phenotype in macrophages (63). Importantly, we observed also a significant decrease in the number of embryos with cords following RFB treatment in infected zebrafish. It is worth highlighting that in the presence of RFB, there is no change in the number of embryos with cords between 2 and 4 dpi, implying that while RFB does not degrade or modify the bacterial cord structure, it likely prevents the formation of additional cords. Moreover, the effect of RFB on cord reduction is particularly interesting as it may prevent the subsequent formation of abscesses (14), considered as a marker of severity of the disease. Consistent with this hypothesis, a marked decrease in abscess formation was observed in RFB-treated zebrafish embryos. Overall, this work supports the practicality of zebrafish as a pre-clinical model to evaluate in real-time the bactericidal efficacy of RFB against M. abscessus infection in the sole context of innate immunity.

482

483

484

485

486 487

488

489

490

491

492

493

494

495

Downloaded from http://aac.asm.org/ on August 22, 2020 at Dana Medical Library, University of Vermont

In summary, although there is a clear lack of bactericidal activity of drugs against M. abscessus (64), these findings support the high activity of RFB against M. abscessus in vivo and in vitro. Our results further emphasize the efficacy of RFB against both extracellular and intracellular forms of M. abscessus, both co-existing in infected patients, as well as a protective effect in an animal model of M. abscessus infection. In addition, we have provided further evidence that S and R variants are differentially susceptible to RFB, likely due to the GPL layer, however the MIC values are not predictive of intracellular drug efficacy.

Together with the fact that RFB is an FDA-approved drug that is already used to treat tuberculosis (66) and M. avium infections (67) with favourable pharmacological properties (68), our data strengthen the view that RFB should be considered as a repurposing drug candidate for the treatment of M. abscessus infections. Importantly, recent work has shown that RFB is synergistic in combinations with other antimicrobials such as clarithromycin, imipenem and tigecycline, and significantly improves the activity of imipenem-tedizolid drug combinations (32, 48, 53, 65). Future studies are required to test whether these RFB combinations are effective against M. abscessus pulmonary infections.

Downloaded from http://aac.asm.org/ on August 22, 2020 at Dana Medical Library, University of Vermont

ACKNO	DWLED	GMENTS
-------	--------------	---------------

1	a	7	
7	J	,	

496

- 498 MDJ received a post-doctoral fellowship granted by Labex EpiGenMed, an «Investissements d'avenir»
- 499 program (ANR-10-LABX-12-01). This study was supported by the Association Gregory Lemarchal and
- 500 Vaincre la Mucoviscidose (RIF20180502320) to LK.
- 501 The authors have no conflict of interest to declare.

502 503

REFERENCES

- 504
- Johansen MD, Herrmann J-L, Kremer L. 2020. Non-tuberculous mycobacteria and the rise of 505
- 506 Mycobacterium abscessus. Nat Rev Microbiol. 18:392-407.
- 507 2. Cowman S, van Ingen J, Griffith DE, Loebinger MR. 2019. Non-tuberculous mycobacterial
- pulmonary disease. Eur Respir J 54:1900250. 508
- Jönsson BE, Gilljam M, Lindblad A, Ridell M, Wold AE, Welinder-Olsson C. 2007. Molecular 509
- 510 epidemiology of Mycobacterium abscessus, with focus on cystic fibrosis. J Clin Microbiol
- 45:1497-1504. 511
- Esther CR, Esserman DA, Gilligan P, Kerr A, Noone PG. 2010. Chronic Mycobacterium abscessus 512
- infection and lung function decline in cystic fibrosis. J Cyst Fibros 9:117-123. 513
- Catherinot E, Roux A-L, Macheras E, Hubert D, Matmar M, Dannhoffer L, Chinet T, Morand P, 514
- 515 Poyart C, Heym B, Rottman M, Gaillard J-L, Herrmann J-L. 2009. Acute respiratory failure
- involving an R variant of Mycobacterium abscessus. J Clin Microbiol 47:271–274. 516

- 517 Adekambi T, Sassi M, van Ingen J, Drancourt M. 2017. Reinstating Mycobacterium massiliense and Mycobacterium bolletii as species of the Mycobacterium abscessus complex. Int J Syst Evol 518 519 Microbiol 67:2726-2730.
- 520 7. Koh W-J, Jeon K, Lee NY, Kim B-J, Kook Y-H, Lee S-H, Park YK, Kim CK, Shin SJ, Huitt GA, Daley CL, Kwon OJ. 2011. Clinical significance of differentiation of Mycobacterium massiliense from 521 522 Mycobacterium abscessus. Am J Respir Crit Care Med 183:405-410.
- 523 Howard ST, Rhoades E, Recht J, Pang X, Alsup A, Kolter R, Lyons CR, Byrd TF. 2006. Spontaneous 524 reversion of Mycobacterium abscessus from a smooth to a rough morphotype is associated with 525 reduced expression of glycopeptidolipid and reacquisition of an invasive phenotype. Microbiology (Reading, Engl) 152:1581–1590. 526
- 527 Gutiérrez AV, Viljoen A, Ghigo E, Herrmann J-L, Kremer L. 2018. Glycopeptidolipids, a doubleedged sword of the Mycobacterium abscessus complex. Front Microbiol 9:1145. 528
- 10. Roux A-L, Viljoen A, Bah A, Simeone R, Bernut A, Laencina L, Deramaudt T, Rottman M, Gaillard 529 530 J-L, Majlessi L, Brosch R, Girard-Misguich F, Vergne I, de Chastellier C, Kremer L, Herrmann J-L. 531 2016. The distinct fate of smooth and rough Mycobacterium abscessus variants inside 532 macrophages. Open Biol 6:160185.
- 11. Bernut A, Viljoen A, Dupont C, Sapriel G, Blaise M, Bouchier C, Brosch R, de Chastellier C, 533 534 Herrmann J-L, Kremer L. 2016. Insights into the smooth-to-rough transitioning in Mycobacterium bolletii unravels a functional Tyr residue conserved in all mycobacterial MmpL family members. 535 536 Mol Microbiol 99:866-883.

- 537 12. Sánchez-Chardi A, Olivares F, Byrd TF, Julián E, Brambilla C, Luquin M. 2011. Demonstration of 538 cord formation by rough Mycobacterium abscessus variants: implications for the clinical 539 microbiology laboratory. J Clin Microbiol 49:2293–2295.
- 540 13. Nessar R, Reyrat J-M, Davidson LB, Byrd TF. 2011. Deletion of the mmpL4b gene in the Mycobacterium abscessus glycopeptidolipid biosynthetic pathway results in loss of surface 541 542 colonization capability, but enhanced ability to replicate in human macrophages and stimulate 543 their innate immune response. Microbiology (Reading, Engl) 157:1187–1195.
- 14. Bernut A, Herrmann J-L, Kissa K, Dubremetz J-F, Gaillard J-L, Lutfalla G, Kremer L. 2014. 544 545 Mycobacterium abscessus cording prevents phagocytosis and promotes abscess formation. Proc Natl Acad Sci USA 111:E943-952. 546
- 547 15. Park IK, Hsu AP, Tettelin H, Shallom SJ, Drake SK, Ding L, Wu U-I, Adamo N, Prevots DR, Olivier KN, Holland SM, Sampaio EP, Zelazny AM. 2015. Clonal diversification and changes in lipid traits 548 549 and colony morphology in Mycobacterium abscessus clinical isolates. J Clin Microbiol 53:3438-3447. 550
- 16. Pawlik A, Garnier G, Orgeur M, Tong P, Lohan A, Le Chevalier F, Sapriel G, Roux A-L, Conlon K, 551 552 Honoré N, Dillies M-A, Ma L, Bouchier C, Coppée J-Y, Gaillard J-L, Gordon SV, Loftus B, Brosch R, 553 Herrmann JL. 2013. Identification and characterization of the genetic changes responsible for characteristic smooth-to-rough morphotype alterations of clinically 554 555 Mycobacterium abscessus. Mol Microbiol 90:612-629.

- 556 17. Madani A, Ridenour JN, Martin BP, Paudel RR, Abdul Basir A, Le Moigne V, Herrmann J-L, 557 Audebert S, Camoin L, Kremer L, Spilling CD, Canaan S, Cavalier J-F. 2019. Cyclipostins and Cyclophostin analogues as multitarget inhibitors that impair growth of Mycobacterium 558 abscessus. ACS Infect Dis 5:1597-1608. 559
- 560 18. Lavollay M, Dubée V, Heym B, Herrmann J-L, Gaillard J-L, Gutmann L, Arthur M, Mainardi J-L. 561 2014. In vitro activity of cefoxitin and imipenem against Mycobacterium abscessus complex. Clin Microbiol Infect 20:0297-0300. 562
- 19. Nessar R, Cambau E, Reyrat JM, Murray A, Gicquel B. 2012. Mycobacterium abscessus: a new 563 564 antibiotic nightmare. J Antimicrob Chemother 67:810-818.
- 20. van Ingen J, Boeree MJ, van Soolingen D, Mouton JW. 2012. Resistance mechanisms and drug 565 566 susceptibility testing of nontuberculous mycobacteria. Drug Resist Updat 15:149-161.
- 567 21. Brown-Elliott BA, Nash KA, Wallace RJ. 2012. Antimicrobial susceptibility testing, drug resistance 568 mechanisms, and therapy of infections with nontuberculous mycobacteria. Clin Microbiol Rev 569 25:545-582.
- 570 22. Lopeman R, Harrison J, Desai M, Cox J. 2019. Mycobacterium abscessus: Environmental 571 bacterium turned clinical nightmare. Microorganisms 7:90.
- 572 23. Luthra S, Rominski A, Sander P. 2018. The role of antibiotic-target-modifying and antibiotic-573 modifying enzymes in Mycobacterium abscessus drug resistance. Front Microbiol 9:2179.

- 574 24. Wu M-L, Aziz DB, Dartois V, Dick T. 2018. NTM drug discovery: status, gaps and the way forward. 575 Drug Discov Today 23:1502-1519.
- 25. Griffith DE, Aksamit T, Brown-Elliott BA, Catanzaro A, Daley C, Gordin F, Holland SM, Horsburgh 576 577 R, Huitt G, Iademarco MF, Iseman M, Olivier K, Ruoss S, von Reyn CF, Wallace RJ, Winthrop K, ATS Mycobacterial Diseases Subcommittee, American Thoracic Society, Infectious Disease 578 579 Society of America. 2007. An official ATS/IDSA statement: diagnosis, treatment, and prevention of nontuberculous mycobacterial diseases. Am J Respir Crit Care Med 175:367–416. 580
- 26. Floto RA, Olivier KN, Saiman L, Daley CL, Herrmann J-L, Nick JA, Noone PG, Bilton D, Corris P, 581 582 Gibson RL, Hempstead SE, Koetz K, Sabadosa KA, Sermet-Gaudelus I, Smyth AR, van Ingen J, Wallace RJ, Winthrop KL, Marshall BC, Haworth CS. 2016. US Cystic Fibrosis Foundation and 583 584 European Cystic Fibrosis Society consensus recommendations for the management of non-585 tuberculous mycobacteria in individuals with cystic fibrosis: executive summary. Thorax 71:88-586 90.
- 27. Daley CL, Jaccarino JM, Lange C, Cambau E, Wallace RJ, Andrejak C, Böttger EC, Brozek J, Griffith 587 DE, Guglielmetti L, Huitt GA, Knight SL, Leitman P, Marras TK, Olivier KN, Santin M, Stout JE, 588 Tortoli E, van Ingen J, Wagner D, Winthrop KL. 2020. Treatment of nontuberculous 589 590 mycobacterial pulmonary disease: an official ATS/ERS/ESCMID/IDSA clinical practice guideline. 591 Eur Respir J 56:2000535.
- 592 28. Wallace RJ, Dukart G, Brown-Elliott BA, Griffith DE, Scerpella EG, Marshall B. 2014. Clinical 593 experience in 52 patients with tigecycline-containing regimens for salvage treatment of

611

612

Chemother 72:376-384.

594 Mycobacterium abscessus and Mycobacterium chelonae infections. J Antimicrob Chemother 69:1945-1953. 595 29. Roux A-L, Catherinot E, Soismier N, Heym B, Bellis G, Lemonnier L, Chiron R, Fauroux B, Le 596 597 Bourgeois M, Munck A, Pin I, Sermet I, Gutierrez C, Véziris N, Jarlier V, Cambau E, Herrmann J-L, Guillemot D, Gaillard J-L, OMA group. 2015. Comparing Mycobacterium massiliense and 598 599 Mycobacterium abscessus lung infections in cystic fibrosis patients. J Cyst Fibros 14:63–69. 600 30. Daniel-Wayman S, Abate G, Barber DL, Bermudez LE, Coler RN, Cynamon MH, Daley CL, Davidson RM, Dick T, Floto RA, Henkle E, Holland SM, Jackson M, Lee RE, Nuermberger EL, 601 602 Olivier KN, Ordway DJ, Prevots DR, Sacchettini JC, Salfinger M, Sassetti CM, Sizemore CF, 603 Winthrop KL, Zelazny AM. 2019. Advancing translational science for pulmonary nontuberculous mycobacterial infections. A road map for research. Am J Respir Crit Care Med 199:947-951. 604 605 31. Aziz DB, Low JL, Wu M-L, Gengenbacher M, Teo JWP, Dartois V, Dick T. 2017. Rifabutin is active 606 against Mycobacterium abscessus complex. Antimicrob Agents Chemother. 61:e00155-17. 607 32. Pryjma M, Burian J, Thompson CJ. 2018. Rifabutin acts in synergy and is bactericidal with frontline Mycobacterium abscessus antibiotics clarithromycin and tigecycline, suggesting a 608 609 potent treatment combination. Antimicrob Agents Chemother 62:e00283-18.

33. Rominski A, Roditscheff A, Selchow P, Böttger EC, Sander P. 2017. Intrinsic rifamycin resistance

of Mycobacterium abscessus is mediated by ADP-ribosyltransferase MAB 0591. J Antimicrob

629

630

613 34. Dick T, Shin SJ, Koh W-J, Dartois V, Gengenbacher M. 2019. Rifabutin is active against Mycobacterium abscessus in mice. Antimicrob Agents Chemother 64:e01943-19. 614 35. Singh S, Bouzinbi N, Chaturvedi V, Godreuil S, Kremer L. 2014. In vitro evaluation of a new drug 615 616 combination against clinical isolates belonging to the Mycobacterium abscessus complex. Clin Microbiol Infect 20:01124-1127. 617 36. Halloum I, Viljoen A, Khanna V, Craig D, Bouchier C, Brosch R, Coxon G, Kremer L. 2017. 618 619 Resistance to thiacetazone derivatives active against Mycobacterium abscessus involves mutations in the MmpL5 transcriptional repressor MAB 4384. Antimicrob Agents Chemother 620 621 61:e02509-16. 37. Woods, GL, Brown-Elliott, BA, Conville, PS, Desmond, EP, Hall, GS, Lin G, Pfyffer GE, Ridderhof, 622 623 JC, Siddiqi, SH, Wallace, RJ. 2011. Susceptibility testing of mycobacteria, nocardiae and other 624 aerobic actinomycetes: approved standardSecond Edition. M24-A2. Clinical and Laboratory 625 Standards Institute, Wayne, PA 2011. 626 38. Lamason RL, Mohideen M-APK, Mest JR, Wong AC, Norton HL, Aros MC, Jurynec MJ, Mao X, Humphreville VR, Humbert JE, Sinha S, Moore JL, Jagadeeswaran P, Zhao W, Ning G, 627

Makalowska I, McKeigue PM, O'donnell D, Kittles R, Parra EJ, Mangini NJ, Grunwald DJ, Shriver

MD, Canfield VA, Cheng KC. 2005. SLC24A5, a putative cation exchanger, affects pigmentation in

zebrafish and humans. Science 310:1782-1786.

- 631 39. Bernut A, Dupont C, Sahuguet A, Herrmann J-L, Lutfalla G, Kremer L. 2015. Deciphering and imaging pathogenesis and cording of Mycobacterium abscessus in zebrafish embryos. J Vis Exp 632
- 633 103:e53130.
- 634 40. Bernut A, Le Moigne V, Lesne T, Lutfalla G, Herrmann J-L, Kremer L. 2014. In vivo assessment of
- drug efficacy against Mycobacterium abscessus using the embryonic zebrafish test system. 635
- 636 Antimicrob Agents Chemother 58:4054-4063.
- 41. Lefebvre A-L, Dubée V, Cortes M, Dorchêne D, Arthur M, Mainardi J-L. 2016. Bactericidal and 637
- 638 intracellular activity of β-lactams against Mycobacterium abscessus. J Antimicrob Chemother
- 71:1556-1563. 639
- 42. Story-Roller E, Maggioncalda EC, Lamichhane G. 2019. Select β-lactam combinations exhibit 640
- synergy against Mycobacterium abscessus in vitro. Antimicrob Agents Chemother 63:e00614-19. 641
- 43. Medjahed H, Reyrat J-M. 2009. Construction of Mycobacterium abscessus defined 642
- glycopeptidolipid mutants: comparison of genetic tools. Appl Environ Microbiol 75:1331–1338. 643
- 44. Roux A-L, Ray A, Pawlik A, Medjahed H, Etienne G, Rottman M, Catherinot E, Coppée J-Y, Chaoui 644
- K, Monsarrat B, Toubert A, Daffé M, Puzo G, Gaillard J-L, Brosch R, Dulphy N, Nigou J, Herrmann 645
- J-L. 2011. Overexpression of proinflammatory TLR-2-signalling lipoproteins in hypervirulent 646
- mycobacterial variants. Cell Microbiol 13:692-704. 647
- 648 45. Ripoll F, Pasek S, Schenowitz C, Dossat C, Barbe V, Rottman M, Macheras E, Heym B, Herrmann
- 649 J-L, Daffé M, Brosch R, Risler J-L, Gaillard J-L. 2009. Non mycobacterial virulence genes in the
- genome of the emerging pathogen Mycobacterium abscessus. PLoS ONE 4:e5660. 650

- 651 46. Balganesh M, Dinesh N, Sharma S, Kuruppath S, Nair AV, Sharma U. 2012. Efflux pumps of
- 652 Mycobacterium tuberculosis play a significant role in antituberculosis activity of potential drug
- 653 candidates. Antimicrob Agents Chemother 56:2643–2651.
- 654 47. Dupont C, Viljoen A, Thomas S, Roquet-Banères F, Herrmann J-L, Pethe K, Kremer L. 2017.
- Bedaguiline inhibits the ATP synthase in Mycobacterium abscessus and is effective in infected 655
- 656 zebrafish. Antimicrob Agents Chemother 61:e01225-17.
- Cheng A, Tsai Y-T, Chang S-Y, Sun H-Y, Wu U-I, Sheng W-H, Chen Y-C, Chang S-C. 2019. In vitro 657
- synergism of rifabutin with clarithromycin, imipenem, and tigecycline against the 658
- 659 Mycobacterium abscessus complex. Antimicrob Agents Chemother 63:e02234-18.
- 660 49. Luna-Herrera J, Reddy MV, Gangadharam PRJ. 1995. In vitro and intracellular activity of rifabutin
- on drug-susceptible and multiple drug-resistant (MDR) tubercle bacilli. J Antimicrob Chemother 661
- 36:355-363. 662
- 50. Dubée V, Bernut A, Cortes M, Lesne T, Dorchene D, Lefebvre A-L, Hugonnet J-E, Gutmann L, 663
- 664 Mainardi J-L, Herrmann J-L, Gaillard J-L, Kremer L, Arthur M. 2015. β-Lactamase inhibition by
- avibactam in Mycobacterium abscessus. J Antimicrob Chemother 70:1051–1058. 665
- 51. Baysarowich J, Koteva K, Hughes DW, Ejim L, Griffiths E, Zhang K, Junop M, Wright GD. 2008. 666
- 667 Rifamycin antibiotic resistance by ADP-ribosylation: Structure and diversity of Arr. Proc Natl
- Acad Sci USA 105:4886-4891. 668
- 52. Ganapathy US, Dartois V, Dick T. 2019. Repositioning rifamycins for Mycobacterium abscessus 669
- 670 lung disease. Expert Opin Drug Discov 1–12.

- 671 53. Le Run E, Arthur M, Mainardi J-L. 2018. In vitro and intracellular activity of imipenem combined
- 672 with rifabutin and avibactam against Mycobacterium abscessus. Antimicrob Agents Chemother
- 673 62:e00623-18.
- 54. Brambilla C, Llorens-Fons M, Julián E, Noguera-Ortega E, Tomàs-Martínez C, Pérez-Trujillo M, 674
- 675 Byrd TF, Alcaide F, Luquin M. 2016. Mycobacteria clumping increase their capacity to damage
- 676 macrophages. Front Microbiol 7:1562.
- 55. Jagielski T, Bakuła Z, Brzostek A, Minias A, Stachowiak R, Kalita J, Napiórkowska A, 677
- Augustynowicz-Kopeć E, Żaczek A, Vasiliauskiene E, Bielecki J, Dziadek J. 2018. Characterization 678
- 679 of mutations conferring resistance to rifampin in Mycobacterium tuberculosis clinical strains.
- Antimicrob Agents Chemother 62:e01093-18. 680
- 56. Richard M, Gutiérrez AV, Viljoen AJ, Ghigo E, Blaise M, Kremer L. 2018. Mechanistic and 681
- 682 structural insights into the unique TetR-dependent regulation of a drug efflux pump in
- 683 Mycobacterium abscessus. Front Microbiol 9:649.
- 57. Richard M, Gutiérrez AV, Viljoen A, Rodriguez-Rincon D, Roquet-Baneres F, Blaise M, Everall I, 684
- Parkhill J, Floto RA, Kremer L. 2019. Mutations in the MAB_2299c TetR regulator confer cross-685
- 686 resistance to clofazimine and bedaquiline in Mycobacterium abscessus. Antimicrob Agents
- Chemother 63:e01316-18. 687
- 58. Gutiérrez AV, Richard M, Roquet-Banères F, Viljoen A, Kremer L. 2019. The TetR-family 688
- transcription factor MAB_2299c regulates the expression of two distinct MmpS-MmpL efflux 689

- 690 pumps involved in cross-resistance to clofazimine and bedaquiline in Mycobacterium abscessus.
- Antimicrob Agents Chemother. 63:e01000-19. 691
- 59. Koteva K, Cox G, Kelso JK, Surette MD, Zubyk HL, Ejim L, Stogios P, Savchenko A, Sørensen D, 692
- Wright GD. 2018. Rox, a rifamycin resistance enzyme with an unprecedented mechanism of 693
- action. Cell Chemical Biology 25:403-412.e5. 694
- 695 60. Lefebvre A-L, Le Moigne V, Bernut A, Veckerlé C, Compain F, Herrmann J-L, Kremer L, Arthur M,
- Mainardi J-L. 2017. Inhibition of the β -lactamase BlaMab by avibactam improves the *in vitro* and 696
- in vivo efficacy of imipenem against Mycobacterium abscessus. Antimicrob Agents Chemother 697
- 698 61:e02440-16.
- 61. Marshall VP, Cialdella JI, Ohlmann GM, Gray GD. 1983. MIC values do not predict the 699
- 700 intraphagocytic killing of Staphylococcus aureus by naphthalenic ansamycins. J Antibiot
- 36:1549-1560. 701
- 702 62. Viljoen A, Viela F, Kremer L, Dufrêne YF. 2020. Fast chemical force microscopy demonstrates
- 703 that glycopeptidolipids define nanodomains of varying hydrophobicity on mycobacteria.
- 704 Nanoscale Horiz 5:944-953.
- 705 63. Halloum I, Carrère-Kremer S, Blaise M, Viljoen A, Bernut A, Le Moigne V, Vilchèze C, Guérardel Y,
- 706 Lutfalla G, Herrmann J-L, Jacobs WR, Kremer L. 2016. Deletion of a dehydratase important for
- 707 intracellular growth and cording renders rough Mycobacterium abscessus avirulent. Proc Natl
- 708 Acad Sci USA 113:E4228-4237.

- 64. Maurer FP, Bruderer VL, Ritter C, Castelberg C, Bloemberg GV, Böttger EC. 2014. Lack of 709
- 710 antimicrobial bactericidal activity in Mycobacterium abscessus. Antimicrob Agents Chemother
- 711 58:3828-3836.
- 712 65. Le Run E, Arthur M, Mainardi J-L. 2019. In vitro and intracellular activity of imipenem combined
- 713 with tedizolid, rifabutin, and avibactam against Mycobacterium abscessus. Antimicrob Agents
- 714 Chemother 63:e01915-18.
- 715 66. Lee H, Ahn S, Hwang NY, Jeon K, Kwon OJ, Huh HJ, Lee NY, Koh W-J. 2017. Treatment outcomes
- of rifabutin-containing regimens for rifabutin-sensitive multidrug-resistant pulmonary 716
- 717 tuberculosis. Int J Infect Dis 65:135-141.
 - 718 67. Griffith DE. 2018. Treatment of Mycobacterium avium complex (MAC). Semin Respir Crit Care
 - 719 Med 39:351-361.
 - 720 68. Blaschke TF, Skinner MH. 1996. The clinical pharmacokinetics of rifabutin. Clin Infect Dis 22
- Suppl 1:S15-21; discussion S21-22. 721

Antimicrobial Agents and Chemotherapy

Table 1. Drug susceptibility/resistance profile of smooth and rough variants derived from the reference *M. abscessus* 104536^T strain to various rifamycins in CaMBH. MIC (μg/mL) were determined following the CLSI guidelines.

				MIC (μg/	mL)
Strain I	Morphotype	RFB	RIF	RPT	RFX
CIP104536 (S)	S	64	>128	>128	>128
CIP104536 (R)	R	16	>128	>128	>128
ΔMAB_mmpL4b	R	16	>128	>128	>128
ΔMAB_mmpL4b_C	S	32	>128	>128	>128
CIP104536 (S) + pMV306- <i>MAB_1409c</i> -	HA S	64	>128	>128	>128
CIP104536 (R) + pMV306- <i>MAB_1409c</i> -	HA R	64	>128	>128	>128

RFB, Rifabutin; RIF, rifampicin; RPT, rifapentine; RFX, rifaximin.

Antimicrobial Agents and Chemotherapy

Table 2. Comparison of the activity of RFB against clinical isolates from CF and non-CF patients. The MIC (µg/mL) was determined in Cation-Adjusted Mueller-Hinton broth for different subspecies belonging to the M. abscessus complex. Results are from 3 independent experiments. RFB, rifabutin.

Strain	Morphotype	Source	RFB
M. abscessus			
CIP104536	S	Non-CF	50
3321	S	Non-CF	50
1298	S	CF	50
2587	S	CF	100
2069	S	Non-CF	100
CF	S	CF	25
2524	R	CF	25
2648	R	CF	25
3022	R	Non-CF	50
5175	R	CF	25
CIP104536	R	Non-CF	25
M. massiliense			
CIP108297	R	Addison Disease	50
210	R	CF	100
179	R	CF	100
CIP108297	S	Addison Disease	100
140	S	CF	50
185	S	CF	100
107	S	CF	50
122	S	CF	100
120	S	CF	6.25
212	S	CF	100
100	S	CF	100
111	S	CF	100
M. bolletii			
CIP108541	S	Non reported	100
114	S	CF	100
17	S	CF	50
116	S	CF	100
97	S	CF	100
112	R	CF	100
19	R	Non-CF	50
10	R	Non reported	100
108	R	CF	25

748 749

750

751 752

753

Table 3. Characterisitics of spontaneous RFB-resistant mutants of M. abscessus. MIC (µg/mL) were determined in Cation-adjusted Mueller-Hinton broth. Resistant strains were derived from the rough M. abscessus CIP104536^T parental strain on Middlbrook 7H10 supplemented with either 25 or 50 μg/mL RFB. Single nucleotide polymorphism identification in rpoB (MAB_3869c) and corresponding amino acid changes are also indicated. RFB, rifabutin.

	MIC (μg/ml)	Mutation in rpoB		
		SNP	AA change	
CIP104536 ^T (R)	12.5	-	-	
25.1	50	C1339T	H447Y	
25.2	100	C1339G	H447D	
50.1	50	C1339T	H447Y	
50.2	50	C1355T	S452L	

FIGURE LEGENDS

Figure 1. In vitro activity of rifabutin. M. abscessus CIP104536^T S (left panel) or R (right panel) was exposed either to 200, 100, 50, 25, 12.5 or 6.25 µg/mL RFB or 16 µg/mL IPM in CaMHB at 30°C. At various time points, bacteria were plated on LB agar and further incubated at 30°C for 4 days prior to CFU counting. Results are expressed as the mean of triplicates ± SD and are representative of two independent experiments. * $P \le 0.05$, ** $P \le 0.01$.

759 760 761

762 763

764

765

766

767

768

769 770

771 772

773 774

775

776

754

755 756

757

758

Figure 2. Intracellular activity of RFB on M. abscessus-infected THP-1 cells. (A) Macrophages were infected with M. abscessus S-morphotype and (B) R-morphotype expressing tdTomato (MOI of 2:1) for 3 hrs prior to treatment with RIF (50 µg/mL), AMK (50 µg/mL), RFB (12.5 µg/mL) or DMSO. CFU were determined at 0, 1 and 3 dpi. Data are mean values ± SD for three independent experiments. Data were analysed using a one-way ANOVA Kruskal-Wallis test. (C) Percentage of infected THP-1 macrophages at 0, 1 and 3 days post-infection after infection with M. abscessus S or (D) M. abscessus R. Data are mean values ± SD for three independent experiments. Data were analysed using a oneway ANOVA Kruskal-Wallis test. (E) Percentage of S-infected macrophage categories and (F) percentage of R-infected macrophage categories infected with different numbers of bacilli (<5 bacilli; 5-10 bacilli and >10 bacilli). The categories were counted at 0 or at 1 and 3 days post-infection in the absence of antibiotics or in the presence of RIF or AMK at 50 µg/mL, or RFB at 12.5 µg/mL. Values are means ± SD from three independent experiments performed in triplicate. (G) Four immunofluorescent fields were taken at 1 day post-infection showing macrophages infected with M. abscessus expressing Tdtomato (red). The surface and the endolysosomal system of the macrophages were detected using anti-CD63 antibodies (green). The nuclei were stained with DAPI (blue). White arrows indicate individual or aggregate mycobacteria. Scale bar, 20 μ m. ** $P \le 0.01$, *** $P \le 0.001$.

777 778

779

780

781

782

Figure 3. Intracellular activity of RFB on S and R clinical isolates. CFU counts of clinical isolates exposed to 25 and 12.5 µg/mL RFB. Macrophages were infected with M. abscessus (A-B) M. bolletii (C-D) or M. massiliense (E-G) clinical strains belonging to S or R morphotypes at MOI of 2:1 for 3 hrs prior to treatment with 250 µg/mL AMK for 2 hrs to kill extracellular bacteria. Following extensive PBS washes, cells were exposed to 50 µg/mL RIF, 50 µg/mL AMK, 25 or 12.5 µg/mL RFB. CFU were

determined at 0, 1 and 3 days post-infection. Data are mean values ± SD for two independent experiments. Data were analysed using the *t*-test. * $P \le 0.05$, ** $P \le 0.01$, *** $P \le 0.001$.

785 786

787

788

789 790

791

792

793

794

795

796 797

798

799

783

784

Figure 4. Activity of RFB on extracellular and intracellular cords. (A) Total number of cords displayed in 20 fields at 3 days post-infection after infection of macrophages with M. abscessus R variant. Data are mean values ± SD for three independent experiments performed in triplicate. Data were analysed using one tailed Mann Whitney's t-test. (B) Percentage of cords formed either extracellularly or intracellularly. The two categories were counted at 3 days post-infection in the absence of antibiotics or in the presence of 50 μg/mL RIF, 50 μg/mL AMK or 12.5 μg/mL RFB. Extracellular or intracellular cords are highlighted using the indicated colour codes. Values are means ± SD for two independent experiments performed each time in triplicate. (C) Four immunofluorescent fields were taken at 3 days post-infection showing the cords formed extracellularly or within macrophages infected with M. abscessus R variant expressing Tdtomato (red). Macrophages were infected for 3 days in the presence of DMSO, RIF (50 μg/mL), AMK (50 μg/mL) or RFB (12.5 µg/mL). The macrophage surface was stained using anti-CD63 antibodies (green). The nuclei were stained with DAPI (blue). White arrows indicate intracellular cords, while red arrows indicate extracellular cords. Scale bars represent 20 µm. Results represent the average of a total of 120 fields per condition. **** $P \le 0.0001$.

800 801

802

803

804

805

806

807

808 809

810

811

812

Figure 5. RFB displays high bactericidal activity against M. abscessus in an embryonic zebrafish infection model. (A) Groups of uninfected embryos were immersed in water containing increasing concentrations of RFB (ranging from 3.125 to 250 µg/mL) for 4 days. The red bar indicates the duration of treatment. The graph shows the survival of the RFB-treated and untreated (DMSO) embryos over a 12-days period. (B) Zebrafish embryos at 30 hrs post-fertilisation were intravenously infected with approximately 250-300 CFU of M. abscessus CIP104536^T (R variant) expressing tdTomato (n=20-25). A standard PBS injection control was included for each experiment. At 1 dpi, embryos were randomly split into equal groups of approximately 20 embryos per group, and varying concentrations of RFB (5 to 50 µg/mL) were added to the water. DMSO was included as a positive control group. RFB was changed daily after which, embryos were washed twice in fresh embryo water, maintained in embryo water and monitored daily over a 12-days period. Each treatment group Downloaded from http://aac.asm.org/ on August 22, 2020 at Dana Medical Library, University of Vermont

814

815

816

817

818

819

820

821

822 823

824

825

826

827

828

829

830

831

832

833

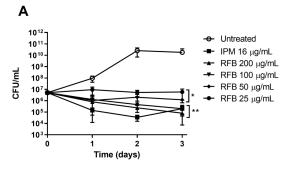
834

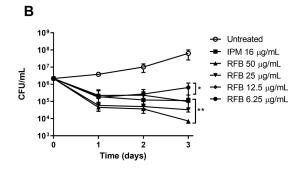
log-rank (Mantel-Cox) statistical test for survival curves. Data shown is the merge of three independent experiments (C) Bacterial burden was determined at 2, 4 and 6 days post-infection following treatment with either DMSO or 50 µg/mL RFB. Bacteria were quantified by fluorescent pixel count determination using ImageJ software, with each data point representing a single embryo. Error bars represent standard deviations. Statistical significance was determined by Student's t-test. The plots represent a pool of 2 independent experiments containing approximately 20-25 embryos per group. (D) Representative embryos from the untreated group (WT) (upper panel) and from the treated group with 50 µg/mL RFB at 6 days post-infection. White arrowheads show tdTomatoexpressing bacteria. Scale bars represent 1 mm. * $P \le 0.05$, *** $P \le 0.001$, **** $P \le 0.0001$. Figure 6. RFB reduces the pathophysiological traits of M. abscessus infection in zebrafish embryos.

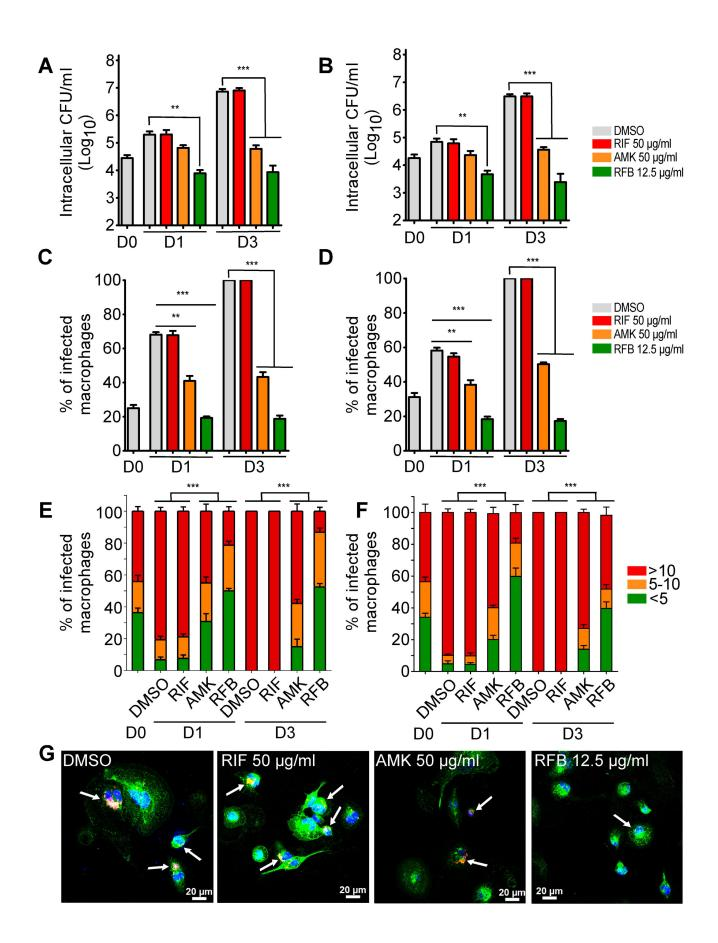
was compared against the untreated infected group with significant differences calculated using the

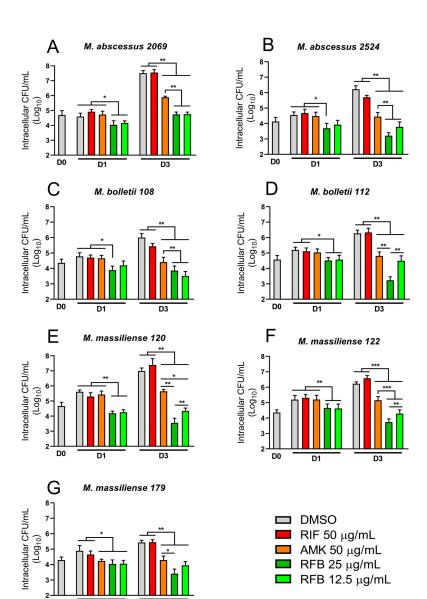
(A) Proportion of embryos with cords at 2 and 4 days post-infection in infected embryos that were either untreated or treated with 50 µg/mL RFB (250-300 CFU, n=30). Data were analysed using an unpaired student's t-test. Data shown is the mean of three independent experiments ± SD. (B) Total percentage of embryos with abscesses at 4 and 6 dpi in infected embryos that were either untreated or treated with 50 µg/mL RFB (250-300 CFU, n=30). Data were analysed using an unpaired student's t-test. Data shown is the mean of three independent experiments ± SD. (C-D) Representative zebrafish images of untreated (WT) embryos and those treated with treated with 50 µg/mL RFB at 6 dpi. Scale bar represents 0.5 mm. White arrows indicate extracellular cords. The white box highlights a large extracellular cord based on the size and morphology, with the scale bar representing 100 μm. Red overlay represents *M. abscessus* expressing tdTomato. * $P \le 0.05$.

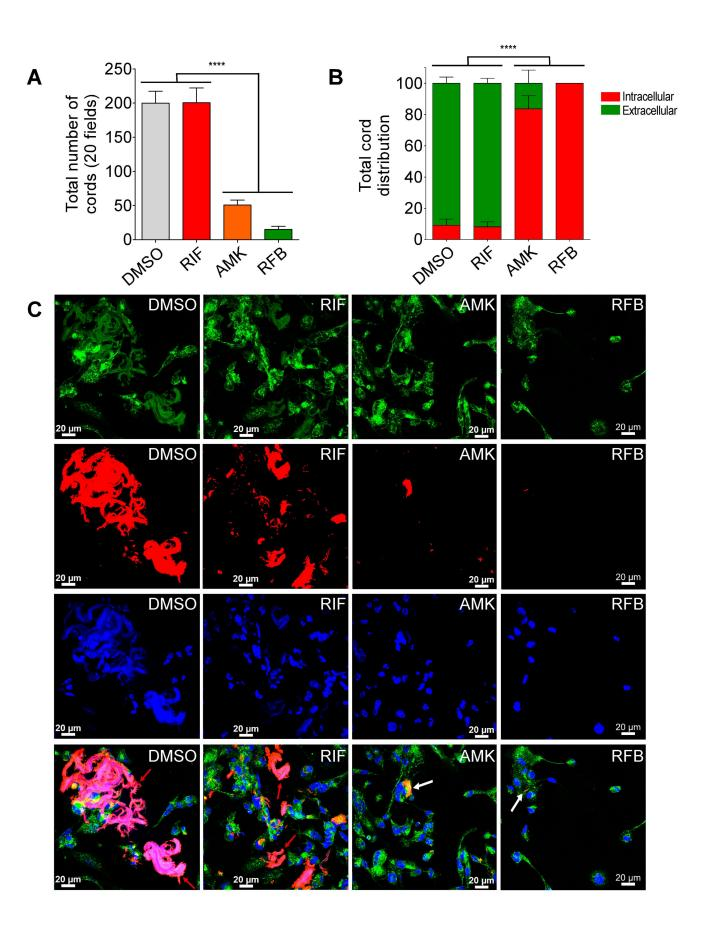
Downloaded from http://aac.asm.org/ on August 22, 2020 at Dana Medical Library, University of Vermont

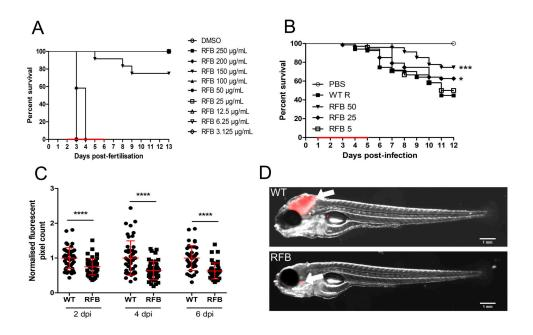








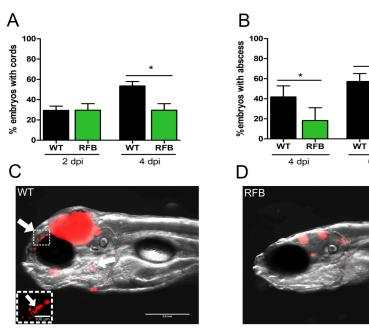












RFB 6 dpi